JOURNAL OF MATERIALS SCIENCE 35 (2000) 1549–1554

# Thermoelectric properties of n-type $SbI_3$-doped $Bi_2Te_{2.85}Se_{0.15}$ compound fabricated by hot pressing and hot extrusion

J. SEO
*Department of Metallurgical Engineering, Inha University, Inchon 402-751, Korea*

C. LEE
*Jointly Appointed at the Center for the Advanced Aerospace Materials, Pohang University of Science and Technology, Pohang 790-784, Korea*

K. PARK
*Department of Materials Engineering, Chung-ju National University, Chungbuk 380-702, Korea*

n-type 0.1 wt% $SbI_3$-doped $Bi_2Te_{2.85}Se_{0.15}$ compounds were fabricated by hot pressing and hot extrusion. The hot pressed compounds were densified up to 99.2% of theoretical density. The grains were preferentially oriented and contained many dislocations due to the hot pressing. The figure of merit of the compounds hot pressed at 420 °C was $2.35 \times 10^{-3}$/K. On the other hand, the grains of the extruded compounds were small, equiaxed, ($\sim$1.0 $\mu$m) and contained many dislocations due to the dynamic recrystallization during the extrusion. The fine grains significantly improved the bending strength and figure of merit. The grains were also preferentially oriented through the extrusion. The bending strength and figure of merit were increased with increasing extrusion temperature. The figure of merit of the compounds hot extruded at 440 °C was $2.62 \times 10^{-3}$/K. 

## 1. Introduction

Bismuth telluride ($Bi_2Te_3$) and its related solid solutions have been used as thermoelectric cooling and heating materials, since they have a high figure of merit at room temperature. The crystal structure of $Bi_2Te_3$ at room temperature is rhombohedral ($a = 0.438$ nm and $c = 3.049$ nm) [1]. This crystal structure is composed of atomic layers in the order of Te/Bi/Te/Te/Bi/Te/Bi/Te/Te/. . . along the *c*-axis. The Te/Te layers are considered to be weakly bound with van der Waal forces [2]. The solid solutions are distinguished by the high degree of anisotropy in most of physical properties. The electrical and mechanical properties along the direction parallel to the cleavage plane are better than those along the direction perpendicular to the plane, i.e., the *c*-axis [3, 4]. As an example, the electrical conductivity of $Bi_2Te_3$ along the direction parallel to the cleavage plane is three to four times as large as that of $Bi_2Te_3$ along the direction perpendicular to the plane.

Owing to the cleavage features, the crystal has low mechanical properties and poor ability in microprocessing for fabricating the miniature thermoelectric modules. It is thus inappropriate for mass production of the thermoelectric modules. Many workers attempted to fabricate the thermoelectric materials without cleavage features. Sintering technique is not effective because the figure of merit of sintered compounds is lower than that of single crystals. It has previously been reported that good n-type materials are the $Bi_2Te_3$-rich solid solutions [5]. The solid solution alloying leads to an increase in the figure of merit ($Z$) owing to the scattering of phonons, which is caused by the disorder in the lattice due to alloying. In this work, we fabricated the n-type $SbI_3$-doped $Bi_2Te_{2.85}Se_{0.15}$ compounds by two different processings, hot pressing and hot extrusion, and then investigated the microstructure and thermoelectric properties of the compounds.

## 2. Experimental

To fabricate the hot-pressed and hot-extruded n-type $Bi_2Te_{2.85}Se_{0.15}$ compounds doped with 0.1 wt% $SbI_3$, the powders of Bi, Te, Se, and $SbI_3$ with >99.99% purity were mixed. The mixture was placed into $SiO_2$ tube with 25 mm diameter and 330 mm length. Then, the tube was evacuated below $10^{-4}$ torr and sealed. The mixture was heated at 700 °C to make a melt. The melt in the tube was stirred under a frequency of 5 times/min at 700 °C for 6 hours using a rocking furnace to make a homogeneous melt without segregation. The tube containing the melt was cooled to room temperature in furnace. The solidified ingot was crushed into fine flakes using $Al_2O_3$ bowl. The resulting flakes were ball milled for 12 hours and then sieved to prepare powders with 45–74 $\mu$m size. To remove the oxygen developed during the crushing and ball milling, the resulting powders

were reduced in hydrogen atmosphere at 360 °C for 4 hours. The powders were compacted by the hot pressing in the temperature range 380 to 420 °C at steps of 20° under 200 MPa in Ar, producing the billets with 30 mm diameter and 6 mm length. Subsequently, the billets hot pressed at 420° and 200 MPa were hot extruded in the temperature range 300–510 °C at steps of 70 °C under an extrusion ratio of 20 : 1 and a ram speed of 50 mm/min.

The density of the hot-pressed and hot-extruded compounds was measured by pycnometer (Micrometric Co.). The mechanical properties were measured at room temperature under a crosshead speed of 0.5 mm/min by three-point bending in accordance with ASTM D790 [6] using a universal testing machine. Detailed microstructural information on the compounds was obtained from transmission electron microscopy (TEM) and X-ray diffraction (XRD). TEM specimens were sectioned from the perpendicular and parallel sections to the processing direction with a low-speed diamond saw. TEM specimens were sectioned from the perpendicular and parallel sections to the processing direction with a low-speed diamond saw. TEM specimens were prepared by mechanical grinding, dimpling, and ion milling. Ion milling was conducted under 1 mA current and 3 kV $Ar^+$ at an incident angle of 12° with liquid nitrogen to minimize ion-induced damage. The microstructure of the specimens was investigated using a Philips CM20 transmission electron microscope.

The thermoelectric properties of the hot-pressed and hot-extruded compounds were measured at room temperature along the directions perpendicular to the pressing direction and parallel to the extrusion direction, respectively. The specimens with dimensions of $2 \times 2 \times 15$ mm and of $4 \times 4 \times 4$ mm were cut out of the compounds for the measurements of the Seebeck coefficient $\alpha$ and thermal conductivity $\kappa$ and of the electrical resistivity $\rho$, respectively. Then, their surfaces were polished with a series of SiC polishing paper of up to #2000 and further polished on a polishing cloth impregnated with $Al_2O_3$ powders of 0.3 $\mu$m size. To measure the Seebeck coefficient $\alpha$, heat was applied to the specimen which was placed between the two Cu discs. The thermoelectric electromotive force $E$ was measured upon applying small temperature difference ($\Delta T < 2\,^\circ$C) between the both ends of the specimen. The Seebeck coefficient $\alpha$ was determined from the $E/\Delta T$. The thermal conductivity $\kappa$ was measured by the static comparative method using a transparent $SiO_2$ ($\kappa = 1.36$ W/Km at room temperature) as a standard sample in $5 \times 10^{-5}$ torr. The electrical resistivity $\rho$ was measured by the four-probe technique. The repeat measurement was made rapidly with a duration smaller than one second to prevent errors due to the Peltier effect.

## 3. Results and discussion

### 3.1. Hot-pressed $Bi_2Te_{2.85}Se_{0.15}$ compounds

It was found that the n-type 0.1 wt% $SbI_3$-doped $Bi_2Te_{2.85}Se_{0.15}$ compounds were relatively dense. The powders of the $Bi_2Te_{2.85}Se_{0.15}$ compounds are flaky so that the flat faces of the powders are contacted by hot pressing. The bonding between the powders became strong with increasing the pressing temperature, resulting in an increase in the density. The densities of the compounds hot pressed at 380, 400, and 420 °C were 97.9, 98.5, and 99.2% of theoretical density, respectively.

Fig. 1 shows the TEM bright field image from the perpendicular section to the hot pressing direction for the compounds hot pressed at 420 °C. The compounds contain many dislocations within grains. The grain size was found to be ~30 $\mu$m. No crystalline defects such as stacking faults and microtwins were observed. The compounds hot pressed at 420 °C showed the bending strength of 51 MPa. The fractograph of the compounds hot pressed at 420 °C is shown in Fig. 2. It is apparent that the fractograph represents transgranular cleavage features. The fracture path follows transgranular cleavage planes. The orientation change from grain to grain is also found.

Fig. 3a and b show the XRD patterns obtained from the perpendicular and parallel sections, respectively, for the compounds hot pressed at 420 °C. The intensity of (0 0 6), (0 0 15), and (0 0 18) planes, which are perpendicular to the *c*-axis, is only observed at the

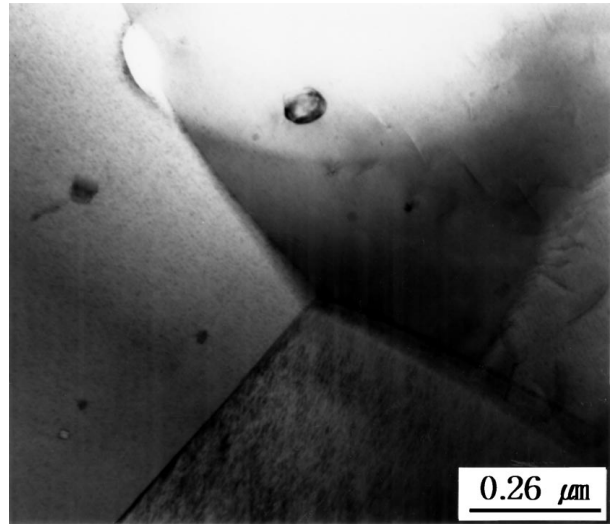


*Figure 1* TEM bright field image from the perpendicular section to the hot pressing direction for the compounds hot pressed at 420 °C.

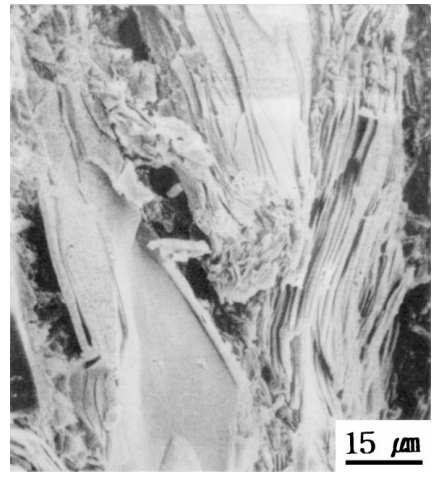


*Figure 2* Fractograph of the compounds hot pressed at 420 °C.

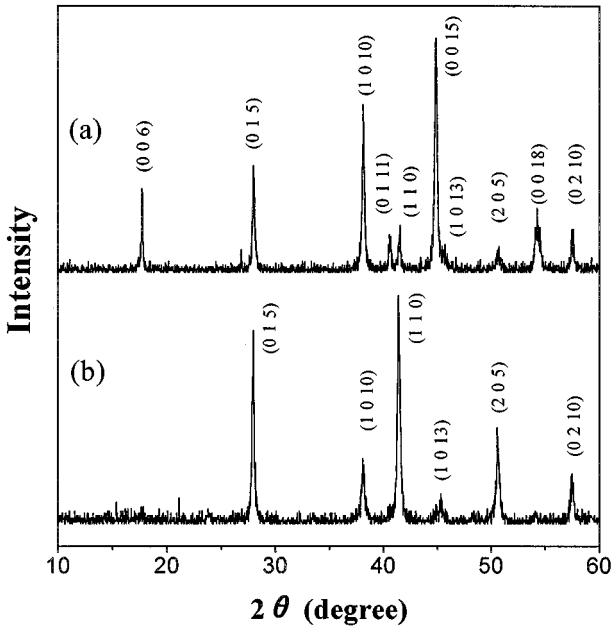


*Figure 3* XRD patterns obtained from the (a) perpendicular and (b) parallel sections to the hot pressing direction for the compounds hot pressed at 420 °C.

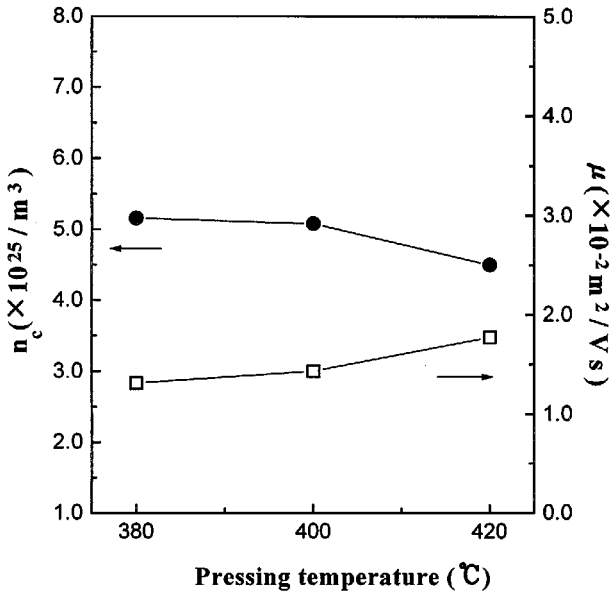


*Figure 4* Carrier concentration $n_c$ and mobility $\mu$ as a function of the hot pressing temperature.

perpendicular section. This indicates that the grains are preferentially oriented through the hot pressing. It has previously been reported that the preferred orientation of grains is observed in unidirectionally solidified materials, in which the growing direction is perpendicular to the *c*-axis [7]. This preferred orientation leads to an increase in the thermoelectric properties.

The carrier concentration $n_c$ and mobility $\mu$ as a function of pressing temperature are shown in Fig. 4. With increasing the pressing temperature, the carrier concentration is slightly decreased, whereas the mobility is increased due to the porosity decrease. At present, the reason for the decrease in carrier concentration is not identified.

The variation of Seebeck coefficient $\alpha$ and electrical resistivity $\rho$ with the pressing temperature is shown in

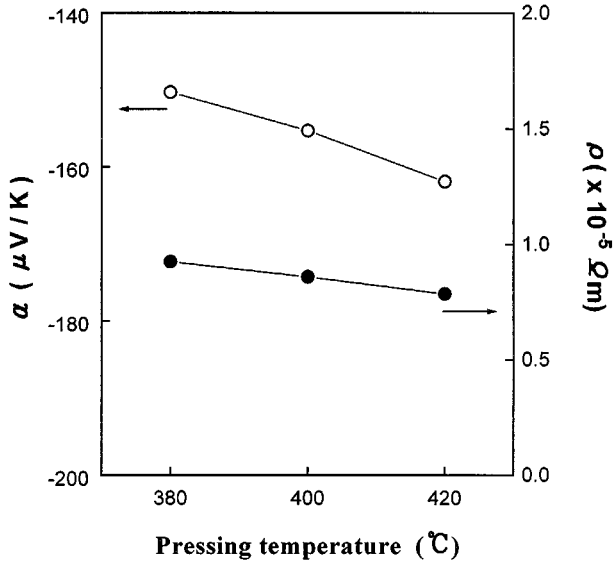


*Figure 5* Variation of the Seebeck coefficient $\alpha$ and electrical resistivity $\rho$ with hot pressing temperature.

Fig. 5. With increasing the pressing temperature, the absolute value of Seebeck coefficient $|\alpha|$ is increased because of the decrease in carrier concentration. The relationship between the $|\alpha|$ and $n_c$ can be expressed as follows:

$$|\alpha| \approx r - \ln n_c \tag{1}$$

where, $r$ is the scattering factor [8]. Also, the electrical resistivity is slightly decreased with the pressing temperature. The electrical resistivity can be expressed as the following relationship:

$$\rho = \frac{1}{n_c e \mu} \tag{2}$$

Consequently, two competing factors, carrier concentration and mobility, determine the electrical resistivity. Therefore, the slight decrease in electrical resistivity would result from the increase in mobility and the slight decrease in carrier concentration. In addition, the thermal conductivity $\kappa$ increased with the pressing temperature probably because of the density increase. The thermal conductivities of the compounds hot pressed at 380, 400, and 420 °C were 1.358, 1.389, and 1.423 W/Km, respectively.

The figure of merit $Z$ was calculated using the following equation:

$$Z = \frac{\alpha^2}{\rho \kappa} \tag{3}$$

Fig. 6 shows the figure of merit $Z$ of the compounds hot pressed at various temperatures. The figure of merit is increased with the pressing temperature. This is because with increasing the pressing temperature, the absolute value of Seebeck coefficient is increased and the electrical resistivity is slightly decreased, although the thermal conductivity is increased. The compounds hot pressed at 420 °C show the figure of merit of $2.35 \times 10^{-3}$/K.

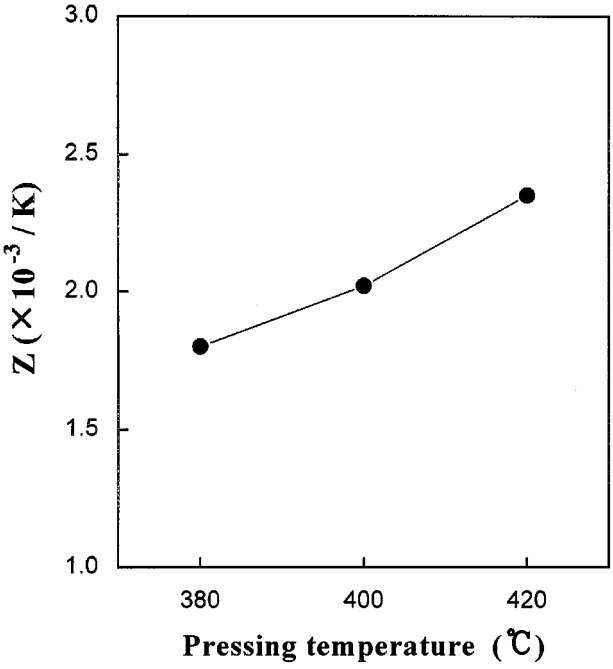


*Figure 6* Figure of merit $Z$ of the compounds hot pressed at various temperatures.

### 3.2. Hot-extruded $Bi_2Te_{2.85}Se_{0.15}$ compounds

The bonding between the powders became strong with increasing the extrusion temperature, giving rise to an increase in the density. The density was achieved up to 99.5% of theoretical density, which was obtained at 440 °C. Also, high-quality extruded bars without any defects such as tearing, orange peel, and blister were obtained in the hot extrusion temperature of 300–440 °C. However, hot cracks were developed during the hot extrusion at 510 °C. This would result from the local melting due to the heat generated by the friction between the billet and die.

Fig. 7a and b show the TEM bright field images from the perpendicular and parallel sections to the extrusion direction, respectively, for the compounds extruded at 440 °C. The crystalline defects such as stacking faults and microtwins were not observed. It is evident that the grains are small equiaxed (∼1.0 $\mu$m) and contain many dislocations because of the dynamic recrystallization (DRX) during the extrusion. The DRX is important for increasing the ductility during the extrusion and for refining the grains. The fine grains significantly improve the product mechanical strength and toughness. The compounds hot extruded at 440 °C showed the bending strength of 95 MPa. The fractograph of the compounds hot extruded at 440 °C is shown in Fig. 8. This figure represents the transgranular cleavage features.

Fig. 9a and b show the XRD patterns obtained from the perpendicular and parallel sections to the extrusion direction, respectively, for the compounds extruded at 440 °C. The intensity of (0 0 6), (0 0 15), and (0 0 18) planes is only observed at the parallel section, strongly indicating that the hot extrusion gave rise to the preferred orientation of grains.

As shown in Fig. 10, with increasing the extrusion temperature, the carrier concentration $n_c$ is decreased

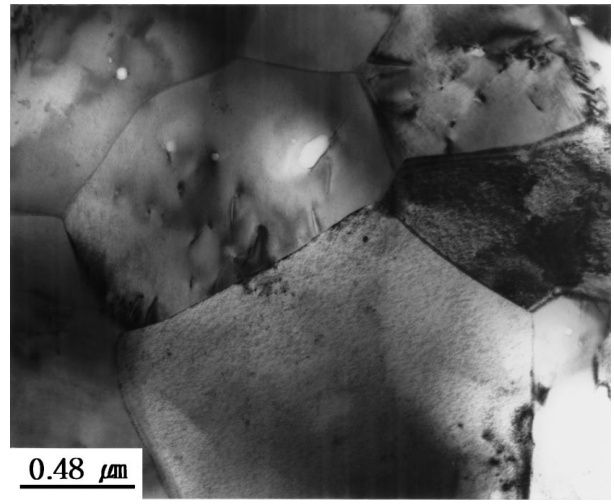


(a)


(b)

*Figure 7* TEM bright field images from the (a) perpendicular and (b) parallel sections to the hot extrusion direction for the compounds hot extruded at 440 °C.

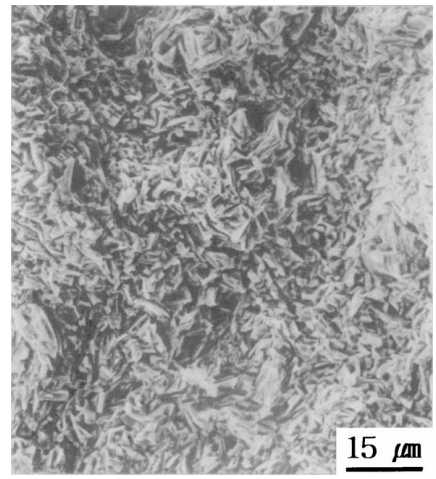


*Figure 8* Fractograph of the compounds hot extruded at 440 °C.

and the mobility $\mu$ is slightly increased due to the porosity decrease. At this time, we do not know the origin of the decrease in carrier concentration. Fig. 11 shows the variation of Seebeck coefficient $\alpha$ and electrical resistivity $\rho$ with the extrusion temperature. This figure represents that the absolute value of Seebeck coefficient

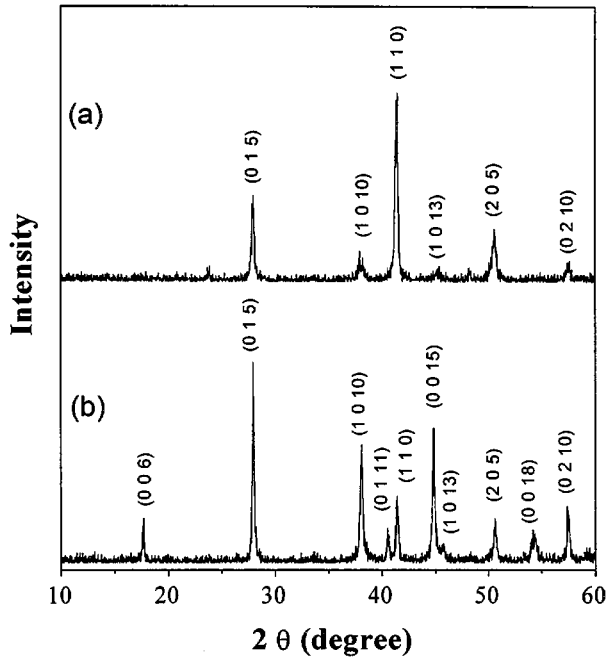


*Figure 9* XRD patterns obtained from the (a) perpendicular and (b) parallel sections to the hot extrusion direction for the compounds hot extruded at 440 °C.

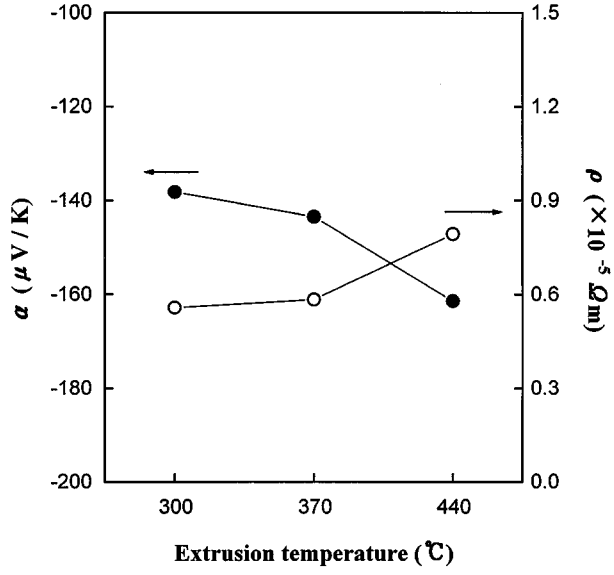


*Figure 11* Variation of the Seebeck coefficient $\alpha$ and electrical resistivity $\rho$ with hot extrusion temperature.

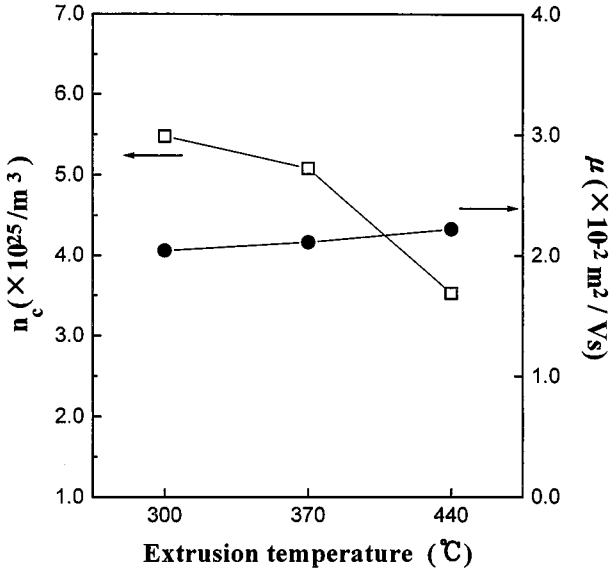


*Figure 10* Carrier concentration $n_c$ and carrier mobility $\mu$ as a function of hot extrusion temperature.

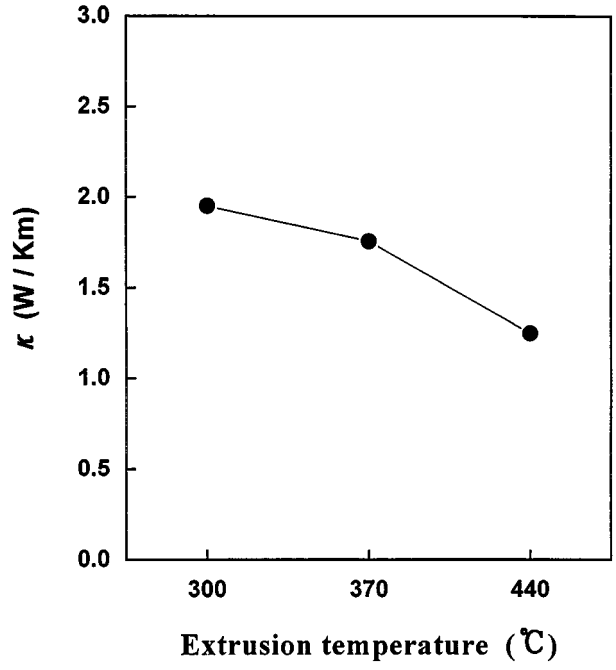


*Figure 12* Relationship between the thermal conductivity $\kappa$ and hot extrusion temperature.

$|\alpha|$ increased with the extrusion temperature probably because of the decrease in carrier concentration. The values of Seebeck coefficient for the compounds hot extruded at 300, 370, and 440 °C are −138.2, −143.4, and −161.5 $\mu$V/K, respectively. Also, the electrical resistivity is increased with the extrusion temperature probably because of the slight increase in mobility and the decrease in carrier concentration. The electrical resistivity of the compounds extruded at 440 °C is $0.798 \times 10^{-5}$ Ω m.

The thermal conductivity $\kappa$ is significantly decreased with increasing the temperature, as shown in Fig. 12. The thermal conductivity (1.249 W/Km) of the compounds hot extruded at 440 °C is much smaller than that of the hot-pressed compounds because of the increase in phonon-grain boundary scattering, which originates from the grain refinement. It has been reported that the phonon-grain boundary scattering has a significant effect on reducing the lattice thermal conductivity of SiGe alloys [9, 10]. The figure of merit $Z$ was calculated using Equation 3. As shown in Fig. 13, the figure of merit increased with the extrusion temperature. This is due to the fact that with increasing the extrusion temperature, the absolute value of Seebeck coefficient is increased and the thermal conductivity is significantly decreased, although the electrical resistivity is increased. The figure of merit of compounds hot extruded at 440 °C is equal to $2.62 \times 10^{-3}$/K.

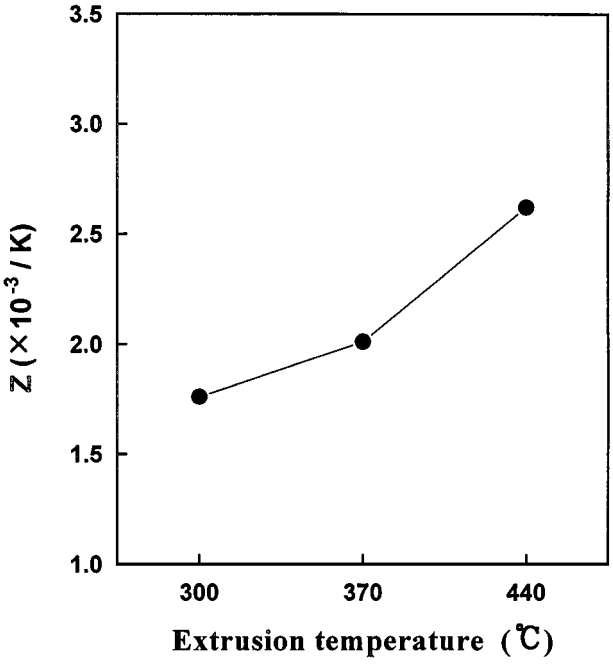


*Figure 13* Figure of merit $Z$ of the compounds hot extruded at various temperatures.

## 4. Conclusions

The n-type 0.1 wt% $SbI_3$-doped $Bi_2Te_{2.85}Se_{0.15}$ compounds fabricated by hot pressing were found to be densified up to 99.2% of theoretical density. The hot pressing gave rise to the preferred orientation of grains. It was also found that the bending strength and the figure of merit increased with increasing the pressing temperature. The bending strength and figure of merit of the compounds hot pressed at 420 °C were 51 MPa and $2.35 \times 10^{-3}$/K, respectively.

On the other hand, the grains of hot-extruded n-type 0.1 wt% $SbI_3$-doped $Bi_2Te_{2.85}Se_{0.15}$ compounds were fine equiaxed ($\sim$1.0 $\mu$m) and contained many dislocations owing to the dynamic recrystallization during the extrusion. The fine grains contribute to an increase in the bending strength and figure of merit. The bending strength of the compounds hot extruded at 440 °C was 97 MPa. Also, the hot extrusion gave rise to the preferred orientation of grains. The highest figure of merit ($2.62 \times 10^{-3}$/K) was obtained at 440 °C. We believe that the extruded compounds could increase the bonding strength between the thermoelectric materials and metal electrode during soldering for the fabrication of thermoelectric modules. The hot extrusion technique is an effective to fabricate the thermoelectric materials with high thermoelectric performance.

## Acknowledgement

We would like to thank the support from the RA scholarship and post doctor program in Inha University.

## References

1. R. W. G. WYCKOFF, "Crystal Structure," Vol. 2 (Interscience Publishers, New York, 1964).
2. J. R. WEISE and L. MULLER, *J. Phys. Chem. Solids* **15** (1960) 13.
3. Y. M. YIM and F. D. ROSI, *Solid State Electronics* **15** (1972) 1121.
4. D. M. ROWE, *Applied Energy* **24** (1986) 139.
5. W. M. YIM, E. V. FITZKE and F. D. ROSI, *J. Mater. Sci.* **1** (1966) 52.
6. ASTM D790, "Standard Test Methods for Flexural Properties of Unreinforced and Reinforced Plastics and Electrical Insulating Materials" (American Society for Testing and Materials, Philadelphia, PA, 1995).
7. J. P. FLEURIAL, L. GAILLIARD, R. TRIBOULET, H. SCHERRER and S. SCHERRER, *J. Phys. Chem. Solids* **49** (1988) 1237.
8. K. UEMURA and I. NISHIDA, "Thermoelectric Semiconductors and Their Application" (Nikkan-Kogyo Shinbun Press, Tokyo, Japan, 1988).
9. H. J. GOLDSMID and A. PENN, *Phys. Lett.* **27A** (1986) 523.
10. J. E. PARROTT, *J. Phys.* **C 2** (1969) 147.

*Received 16 June 1997*
*and accepted 30 September 1999*